AIMS Bioengineering, 9(3): 293–306.
DOI: 10.3934/bioeng.2022020
Received: 26 July 2022
Revised: 03 September 2022
Accepted: 19 September 2022
Published: 21 September 2022

http://www.aimspress.com/journal/Bioengineering

Perspective

Current and future perspectives of atomic force microscopy to elicit the intrinsic properties of soft matter at the single molecule level

Carlos Marcuello[1,2,*]

[1] Institute of Nanoscience and Materials of Aragón (INMA), CSIC-University of Zaragoza, 50018 Zaragoza, Spain
[2] Advanced Microscopy Laboratory (LMA), University of Zaragoza, 50018 Zaragoza, Spain

* **Correspondence:** Email: cmarcuel@unizar.es; Tel: +34876555337.

Abstract: Soft matter encompasses multitude of systems like biomolecules, living cells, polymers, composites or blends. The increasing interest to better understand their physico-chemical properties has significantly favored the development of new techniques with unprecedented resolution. In this framework, atomic force microscopy (AFM) can act as one main actor to address multitude of intrinsic sample characteristics at the nanoscale level. AFM presents many advantages in comparison to other bulk techniques as the assessment of individual entities discharging thus, ensemble averaging phenomena. Moreover, AFM enables the visualization of singular events that eventually can provide response of some open questions that still remain unclear. The present manuscript aims to make the reader aware of the potential applications in the employment of this tool by providing recent examples of scientific studies where AFM has been employed with success. Several operational modes like AFM imaging, AFM based force spectroscopy (AFM-FS), nanoindentation, AFM-nanoscale infrared spectroscopy (AFM-nanoIR) or magnetic force microscopy (MFM) will be fully explained to detail the type of information that AFM is capable to gather. Finally, future prospects will be delivered to discern the following steps to be conducted in this field.

Keywords: atomic force microscopy (AFM); AFM nanoinfrared spectroscopy; biomolecular interactions; biophysics; force spectroscopy; nanoindentation; nanoscale; physico-chemical properties; single molecule studies.

Nowadays, the miniaturization of bioelectronic devices in order to improve their performance, the design of more efficient compounds to exert their function accurately, the fabrication of durable and green-friendly packaging items minimizing the content of scarce based-fossil fuel materials or the precise knowledge of the entire mechanisms which govern biomolecules and cellular systems require the progress of high-throughput techniques. From its discovery [1], atomic force microscopy (AFM) has emerged as promising technique to interrogate multitude of properties from samples with different nature. AFM presents some advantages in comparison to other nanoscale microscopies. AFM does not request the addition of external contrast agents to measure carbon-sourced biological samples like scanning electron microscopy (SEM) or conduct the experiments at ultra-low temperatures as cryo-transmission electron microscopy (cryo-TEM). Furthermore, AFM is capable to devote the measurements at liquid media mimicking the near-physiological conditions inner the living cell. AFM consists of a flexible cantilever where a laser beam is reflected towards a photodetector sensor device. The flexible cantilever ends with a sharp tip which interacts with the external sample surface. The close-loop feedback maintain the setpoint parameter under controlled by modifying the proportional-integral-derivative (PID) settings [2]. Finally, the sample is mounted on a piezoelectric tube made by ceramic materials which are deformed under applied voltages. This fact enables to deliver excellent vertical resolution. AFM treasures multitude of operational modes specialized to acquire one specific property of the sample of interest.

AFM imaging consists to raster the sample with an AFM tip in order to collect topology maps. Today it exists many operational modes to gather the topography information of soft matter systems. Contact mode (CM-AFM) sets the cantilever bending as setpoint and the user can define the grade of interaction between the AFM tip and the scanned sample. Tip-sample interaction is settled by the constant applied force between both surfaces. Alternatively, tapping mode (TM-AFM) controls the oscillation amplitude, the frequency shift or the phase variance as feedback. Here, the tip-sample interaction is based on the AFM cantilever oscillation damping. TM-AFM is considered a semi-intermittent mode that minimizes the non-desirable frictional forces when the AFM probe oscillates with the sufficient amplitude. The main drawbacks experienced for CM-AFM and TM-AFM are the possibility to drag the imaged features during data acquisition in combination with potential sample damage due to the high-lateral forces exerted by the AFM tip and the lack of control of absolute vertical forces that could drive the soft samples compression, respectively. Suppliers have developed other operational modes in order to overcome the aforementioned limitations like peak-force tapping (Bruker) or QI mode (JPK-Bruker). The first mentioned technology monitors the applied AFM tip load forces on the sample surface. This fact enables to preserve the integrity of soft matter systems recording high-quality topography information. Peak force tapping mode has pave the way to evolve peak-force quantitative nanomechanics (PF-QNM) to address the nanomechanical properties of soft samples (See section titled nanoindentation). On the other hand, QI-mode makes negligible the sample invasiveness by efficient algorithms that allows automated tip-sample interaction rendering thus, nondestructive imaging straightforward. All the above described modes display low temporal resolutions (from tens of seconds to minutes scale). High-speed AFM (HS-AFM) through the design of ultra-short cantilevers [3] achieved to work at high-resonance frequencies that leads microseconds acquisition times [4]. Independently of the selected operational mode, imaging always is advisable to choose AFM cantilevers with low spring constants (range of 0.01–0.1 N/m) to gather topology information of soft matter systems.

Table 1 recaps the capabilities of all mentioned AFM imaging modes. AFM imaging succeed to

study the biomolecular morphological changes upon ligand catalysis [5–8] which is relevant to know those conditions where the biomolecule of interest renders the best catalytic performance. Next generation of bioreactors strongly depends on the insights achieved on this regard [9]. In addition, AFM imaging is capable to discern the number of units involved in hepatotoxic strand formation under the presence of certain metal ions [10] or the effect of coniferyl alcohol polymerization by Fenton reaction on bioinspired lignin films [11]. This latest study is relevant to create novel antibacterial films based on plant sourced polymers [12]. The record of biomolecular surface charges [13] or conformational dynamics of ATP synthases [14] and rhodopsin dimers from the G-protein-coupled photoreceptor family [15] under the presence of protons and light, respectively are additional relevant cases that showcase AFM as core technique in this field. The final example of AFM imaging studies is the assessment of the interplay between proteins and DNA chains [16, 17] which can be substantial to devise biomolecular scaffolds [18]. Hence, AFM is a powerful tool to elicit the morphological properties of soft matter systems [19].

Table 1. Comparison between available AFM imaging modes according to the feedback and the main advantages and weaknesses depicted.

Operational mode	Setpoint	Main advantage	Main weakness
CM-AFM	Cantilever bending	High stability	High lateral forces
TM-AFM	Resonance amplitude Frequency shift Phase difference	Low lateral forces	No control vertical force
PF-TM	Applied force (>50 pN)	Constant feedback	Low temp. resolution (~ms)
QI-mode	Deflection of cantilever down to the height of zero force	Constant feedback	Low temp. resolution (~ms)
HS-AFM	Resonance amplitude	High temp. resolution (~μs)	Low scan range

Then, AFM based force spectroscopy (AFM-FS) determines the intra- or intermolecular interactions between biomolecules [20,21]. The classical example of multidomain protein unfolding is the case of titin [22]. The role of redox conditions can lead to prevent and better diagnose cardiac diseases [23]. On the other hand, big efforts have been made to decipher the intermolecular interactions of DNA strands [24], protein-protein [25], cell-cell [26], small molecules like rotaxanes [27], and lignocellulosic polymers with cellulose nanocrystals functionalized AFM levers [28]. The potential industrial applications of the latest described scientific work is the optimization of composite materials by introducing sustainable plant fibers as fillers inside matrices [29]. AFM-FS experiments require proper functionalized strategies [30] by orienting the partner towards the soft matter sample of interest [31]. AFM-FS can become to dynamic force spectroscopy (DFS) by varying the retraction velocity of the AFM cantilever.

Through the Ritchie-Evans equation the dissociation parameters of the system studied can be obtained [32] (1):

$$F^* = \left(\frac{k_B . T}{x_\beta}\right) + ln\left(\frac{R . x_\beta}{k_{off} . k_B . T}\right) \quad (1)$$

where, F^* is the most probable rupture force of one individual analyzed complex, k_B is Boltzmann's contant, T is the absolute temperature, x_β is the distance between the bound state and the energetic maximum, R is the loading rate and k_{off} is the dissociation rate at equilibrium. Thus, x_β and k_{off} dissociation parameters are obtained when the F^* is plotted respect to the neperian logarithm of R. The dissociation parameters have been obtained by DFS for flavoenzimes [33], enzyme-cofactor [34], proteins [35] or peptide-cell membrane receptors [36] complexes, among others. The Ritchie-Evans equation is rooted in the Bell model [37] which in turn is based on the Arrhenius equation or Kramers rate theory (2) [38]:

$$k = k_0 e^{-\Delta U/kT} \quad (2)$$

where, ΔU and k_0 parameters are the variation of the single reaction coordinate and the intrinsic rate, respectively. Kramers rate theory states the free energy barrier ($\Delta G^{\dagger}$) proportionally decreases when external load forces are exerted. Subsequently, these load forces also cause the increase of the bond rupture rate. Conventional AFM setups (except HS-AFM) only provides small range of loading rates which are low. At this regime of loading rates, the mean values of F^* obtained in (1) result from Arrhenius equation of kinetic rate [39]. Thus, it is demonstrated the loading rate dependence and stiffness of the AFM apparatus on the single-dimensional energy landscapes from the chemical bonds of interest [40,41]. Experimental measurements have been carried out to demonstrate this hypothesis. The rupture force of native bonds formed by β1 and β5 polypeptide chains from ubiquitin protein increases with the loading device stiffness when varies from 10 to 1000 pN/m at the same tested AFM lever loading rate [42]. Therefore, Ritchie-Evans equation only is accepted for low regimes of loading rate. When the plot renders one single linear trend means that only exists one energetic barrier when the complex decouples, whereas two linear regimes are related to two different energy landscapes between the bound and the dissociate complexes. Free energies can be also obtained by physical simulations [43]. Recently, some applications have been found in this field like the exploration of the energy landscape of DNA respect to antiviral drugs [44] which will significantly aid to advance in the creation of more effective therapies against human diseases. In addition to binary transient biomolecular complexes, DFS can also be devoted to reconstruct energy landscapes for intramolecular folding events observed in multidomain proteins or nucleic acids [45].

Thereupon, nanoindentation measurements consist in penetrate some nanometers the external sample surface by the AFM tip through applying external force on the AFM cantilever. After recording the force-distance curve, the mechanical deformation underwent by the sample is obtained by the slope of the force profile. Higher slopes are related to stiffer samples, whereas smoother slopes correspond to soft materials [46]. Nanomechanical parameters like the Young's modulus or energy dissipation are obtained by nanoindentation studies. Many theoretical frameworks have been built up to address the Young's modulus of soft matter systems using the AFM tip as nanoindenter. The approaches most used in this field are rooted in Hertz and Derjaguin-Müller-Toporov (DMT) works.

Hertz model hypothesized the nanoindentator geometry is an ideal sphere exerting perpendicular penetration on the studied surface [47]. Hertz model neglects the adhesion forces established between the AFM tip and the sample surface (3).

$$d = \left(\frac{9 F^2}{16 E_{eff}^2 R_{eff}}\right)^{1/3} \quad (3)$$

here, *d* is the indentation depth, *F* is the indentation force, E*eff* is the effective Young's modulus and R_{eff} is the effective curvature radius of the nanoindenter.

The elastic modulus of the soft matter sample of interest can be obtained by (4):

$$\frac{1}{E_{eff}} = \left(\frac{1-\upsilon_T}{E_T}\right) + \left(\frac{1-\upsilon_S}{E_S}\right) \quad (4)$$

being, υ the Poisson's ratio and the subscripts *T* and *S* the AFM tip and sample, respectively. Then, DMT model takes into consideration long-range AFM tip-sample adhesion forces [48]. The Young's modulus of the soft matter system can be achieved by (5):

$$\boldsymbol{E} = \left(\frac{R\ F}{a^3}\right) + (\boldsymbol{F} + \boldsymbol{2\pi R w}) \quad (5)$$

where, *a* is the contact radius between the surfaces of the AFM tip and the indented sample, *F* is the load force applied by the nanoindenter and *w* is the required energy to separate the unit area of both surfaces. Commonly, it is recommended the use of Hertz model when the radius of the AFM tip employed is large, whereas DMT model is broadly conducted for sharp AFM tips. Young's modulus of cells [49], virus capsids [50], cancer cells [51], lignocellulosic films at different relative humidities [52] or hydrogels [53] have been revealed. It has been reported that changes on cellular membrane rigidity affects mechanotransduction processes [54] and proliferation [55] which impacts on the growth of human diseases [56]. On the other hand, revealing the nanomechanical properties of biopolymer films, composites, hydrogels or biotissues serve to acquaint their wettability, rigidity and elastic performance which is crucial to use them for many industrial applications [57].

AFM-nanoscale infrared spectroscopy (AFM-nanoIR) is based on a pulsed, tunable IR laser light aligned to the same scanned area by the commercial AFM tip. The photothermal expansion induced by sample absorption causes the vibration of the chemical bonds involved in the scanned sample surface area being thus, chemically characterized [58]. Two different modes to acquire chemical information of soft matter systems by AFM-nanoIR are available. First, AFM-nanoIR can perform chemical mapping at one defined wavenumber value. This aspect is of enormous importance when the user aims to discriminate between surfaces with different chemistry and it exists previous knowledge about the expected chemical bonds that serve as target. One illustrative example is the characterization of plant cell sections embedded by resins with benchmark wavenumber of 1710 cm^{-1} typical of carboxylic acids coming from the tested resin agents [59]. Chemical mapping offers excellent lateral resolution below 10 nm. The second approach is the "point and shoot" method based on obtaining conventional full IR spectral at specific soft matter sample regions. It is not unusual to observe slightly shifts of the wavenumbers found on the maximum of the IR spectra peaks between nanoscale and bulk measurements. This fact is attributed to the changes underwent by chemical bond lengths that eventually can take place when differences in electronegativity of neighboring atoms are experienced [60]. AFM nanoIR technique has been exploited to locate cell membrane receptors [61], the interrogation of chemical changes observed by the interaction of amyloidogenic proteins involved in neurodegenerative disorders with peptide inhibitors [62] or polymeric blends [63] for the manufacturing of sustainable food packaging or other enveloping items.

Finally, magnetic force microscopy (MFM) measures the magnetic response provided by the sample upon AFM tips coated with cobalt-chromium. Distance between AFM tip and the external sample surface area is fixed at several hundred of nanometers in order to prevent the non-desirable short-range Van der Waals interactions which can interfere during the data acquisition. Repulsive and attractive magnetic forces coming from the sample cause a bend of the flexible cantilever which will

be recorded by the AFM electronic system. Thus, MFM detects local magnetic fields with the classical AFM spatial resolution [64]. Magnetic properties of magnetosome nanoparticles coming from magnetotactic bacteria [65] which could be exploited as microswimmer robots under induced flow fields [66], proteins functionalized with magnetic nanoparticles [67] or magnetic nanoparticles embedded in polymer matrices [68] have been measured by MFM. The main applications of the most relevant outcomes found by MFM are based on hyperthermia [69], drug delivery [70] treatments, development of energy storage devices [71], or emulsion separation in petroleum industry [72], among others. To conclude, AFM is presented as suitable alternative to assess the physico-chemical properties of soft materials. Five different operational modes have been presented to illustrate the potential of this technique (Figure 1) and their potential applications (Figure 2).

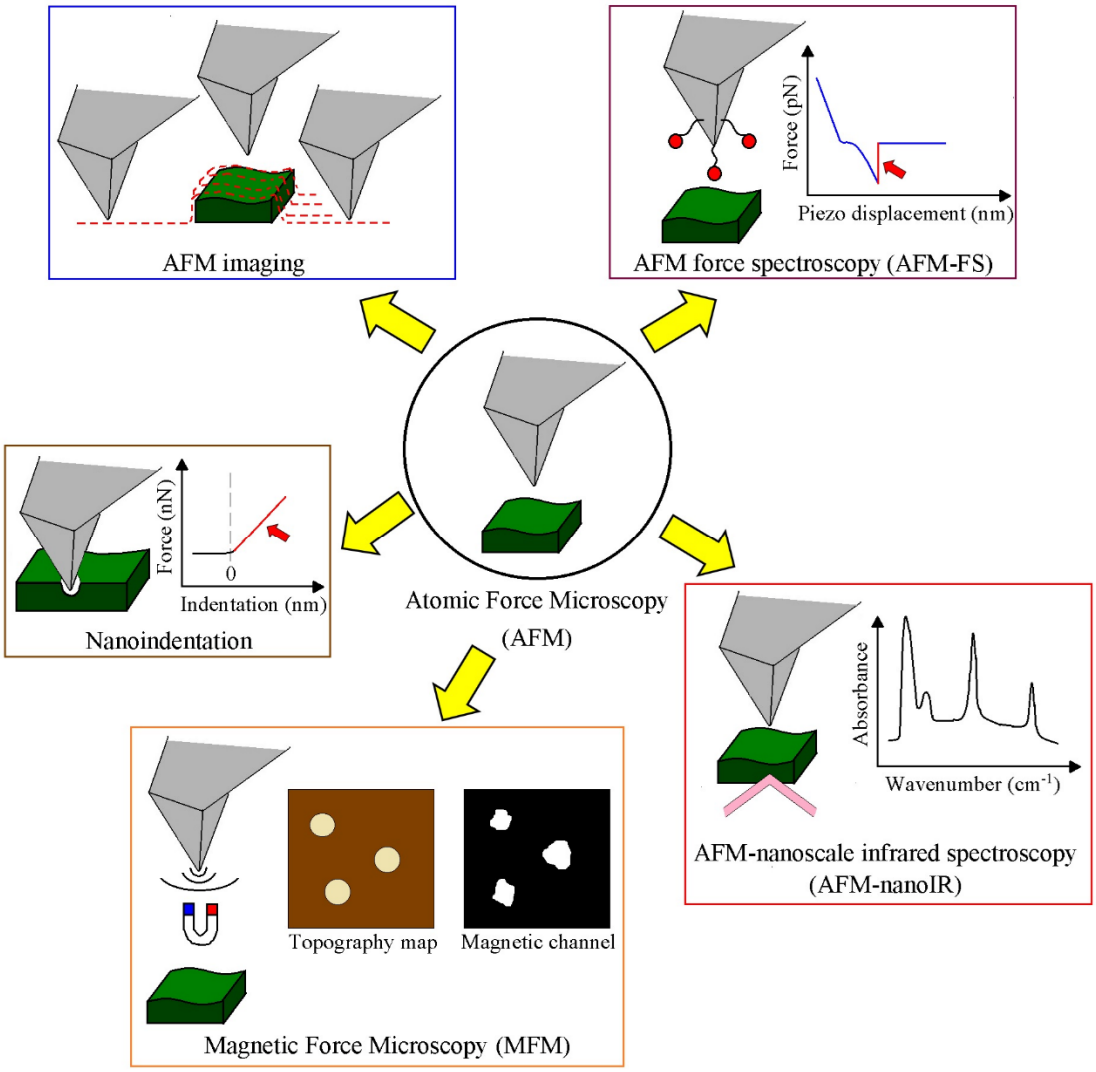

Figure 1. Schematic illustration of atomic force microscopy (AFM) technique highlighted in black circle. AFM imaging (TM-AFM), AFM force spectroscopy (AFM-FS), nanoindentation, AFM-nanoscale infrared spectroscopy (AFM-nanoIR) and magnetic force microscopy (MFM) are remarked in blue, purple, brown, red and orange rectangles, respectively. The adhesion force and young's modulus values are obtained from the regions depicted in red color from their respective force-distance curves.

AFM operational modes	Applications
AFM imaging	• Topography characterization • Biomolecular dynamics • Quality control of blend synthesis
AFM-force spectroscopy	• Adhesion properties of soft matter • Unfolding of nucleic acid strands or multidomain proteins • Dissociation landscapes of molecular complexes
Nanoindentation	• Cellular mechanotransduction processes • Elastic modulus of biopolymers • Monitor changes of material rigidities under external agents
AFM-nanoIR	• Chemical imaging of soft matter • Chemical characterization of local areas • Monitor chemical modifications and reactivity
Magnetic force microscopy	• Interrogation of magnetic performance • Develop more efficient hyperthermia treatments • Design of high-throughput energy storage devices

Figure 2. Some relevant applications of the five addressed AFM operational modes (AFM imaging, AFM-FS, nanoindentation, AFM-nanoIR and MFM, respectively) for Research & Development and Industry fields.

Promising future perspectives are expected in the use of AFM in this field. Volumetric analyses have been developed by defining a mask threshold on topography images obtained by AFM imaging [73]. This aspect facilitate the statistical study of the observed features providing less scattering results. The main limitation to conduct imaging with conventional AFM apparatus is the poor temporal resolution achieved. HS-AFM allows to acquire ultra-fast images that allows to monitor in real-time the change biomolecular dynamic conformations in relevant conditions. The design and fabrication of smaller cantilevers in combination to high-response Z-scanners with the subsequent optimization of hardware and software components will be the basis of the next-generation of HS-AFMs. In this framework, the "only trace imaging" (OTI) mode has been evolved by discharging the record of the backward scan period [74]. OTI mode enables scan rates ranging from 8 frames per second (fps) to 30 fps improving nearby 2.5 times the data acquisition from previous HS-AFMs. Moreover, HS-AFM has recently used in the field of AFM-FS to determine the dissociation parameters of streptavidin:biotin [75]. Streptavidin:biotin system serves as proof-of-concept being the strongest non-covalent complex known in nature. HS-AFM succeed to obtain the information related to the

complex rupture at loading rates more similar than the taken place in the living life organisms. Alternately, the optimization of AFM-FS experiments drives molecular recognition imaging (MRI) studies [76]. MRI simultaneously acquires the topography map and the maximum AFM-tip adhesion force for each pixel of the scanned area being possible to quantitatively correlate the visualized features with their adhesion properties. Moreover, the combination of AFM-FS with Kelvin probe force microscopy can open new avenues in the recognition of soft matter systems by combining specific intermolecular interactions with surface potentials [77]. These quantitative MRI methods significantly improve previous qualitative MRI approaches like AFM-based simultaneous topography and recognition imaging (TREC) [78] where the functional principle is based on the contrast image created between the lower part of the AFM cantilever amplitude oscillation respect to the upper part. The lower and upper parts of the amplitude oscillation yield topography information and molecular recognition images, respectively. Quantitative MRI technologies may open a door in the development of ultrasensitive detection technologies [79]. Furthermore, MRI experiments have shown to map biomolecular alterations like DNA methylation [80] which is relevant to monitor DNA mechanism effects. This technology could be expandable to study the redox functions involved in aging and disease [81]. It is also expected the employment of alternative techniques like computational modeling in combination with AFM can shed light to the physico-chemical properties of soft matter systems [82]. Nevertheless, AFM-FS also needs to deal with challenges, such as the noise threshold limit during sensing soft matter inter-/intramolecular forces which is nearby 15–20 pN. Optical tweezers (OT) [83] and magnetic tweezers (MT) [84] tools have raised to solve this limitation. OT and MT can trap the soft matter sample (typically biomolecules or living cells) by a laser beam source or through magnetic microbeads, respectively. Other advantage presented by OT and MT is the lack of sample immobilization on solid surfaces eliminating detrimental lateral forces during data acquisition. We expect the crosstalk of the five presented AFM operational modes in combination with other complementary single molecule techniques will significantly aid to better understand the underlying mechanisms of soft matter systems at the nanoscale level. This aspect is relevant to assess information that can be hidden in bulk studies like transient phenomena, rare events, conformational changes or crowding effects or local heterogeneities, among others.

Acknowledgments

This research did not receive any specific grant from funding agencies in the public, commercial, or not-for profit sectors. The author acknowledges the funding that covers his salary coming from EU Recovery action 2021 (CSIC - project code: QTP2103003).

Conflict of interest

The author declares no conflict of interest.

Author contributions

Carlos Marcuello contributed in the conceptualization, original draft preparation, validation, writing-review and edition. The author has read and agreed to the published version of the manuscript.

References

1. Binnig G, Quate CF, Gerber C (1986) Atomic force microcopy. *Phys Rev Lett* 56: 930–933. https://doi.org/10.1103/PhysRevLett.56.930
2. Liu H, Li Y, Zhang Y, et al. (2018) Intelligent tuning method of PID parameters based on iterative learning control for atomic force microscopy. *Micron* 104: 26–36. https://doi.org/10.1016/j.micron.2017.09.009
3. Valotteau C, Sumbul F, Rico F (2019) High-speed force spectroscopy: microsecond force measurements using ultrashort cantilevers. *Biophys Rev* 11: 689–699. https://doi.org/10.1007/s12551-019-00585-4
4. Ando T (2018) High-speed atomic force microscopy and its future prospects. *Biophys Rev* 10: 285–292. https://doi.org/10.1007/s12551-017-0356-5
5. Marcuello C, Arilla-Luna S, Medina M, et al. (2013) Detection of a quaternary organization into dimer of trimers of Corynebacterium ammoniagenes FAD synthetase at the single-molecule level and at the in cell level. *Biochim Biophys Acta* 1834: 665–676. https://doi.org/10.1016/j.bbapap.2012.12.013
6. Vega S, Neira JL, Marcuello C, et al. (2013) NS3 protease from hepatitis C virus:biophysical studies on an intrinsically disordered protein domain. *Int J Mol Sci* 14: 13282–13306. https://doi.org/10.3390/ijms140713282
7. Villanueva R, Ferreira P, Marcuello C, et al. (2015) Key residues regulation the reductase activity of the human mitochondrial apoptosis inducing factor. *Biochemistry* 54: 5175–5184. https://doi.org/10.1021/acs.biochem.5b00696
8. Sebastián M, Lira-Navarrete E, Serrano A, et al. (2017) The FAD synthetase from the human pathogen Streptococcus penumoniae: a bifunctional enzyme exhibiting activity-dependent redox requirements. *Sci Rep* 7: 7609. https://doi.org/10.1038/s41598-017-07716-5
9. Song Q, Mao Y, Wilkins M, et al. (2016) Cellulase immobilization on superparamagnetic nanoparticles for reuse in cellulosic biomass conversion. *AIMS Bioeng* 3: 264–276. https://doi.org/10.3934/bioeng.2016.3.264
10. Ceballos-Laita L, Marcuello C, Lostao A, et al. (2017) Microcystin-LR binds Iron, and Iron promotes self-assembly. *Environ Sci Technol* 51: 4841–4850. https://doi.org/10.1021/acs.est.6b05939
11. Gerbin E, Frapart Y-M, Marcuello C, et al. (2020) Dual antioxidant properties and organic radical stabilization in cellulose nanocomposite films functionalized by in situ polymerization of coniferyl alcohol. *Biomacromolecules* 21: 3163–3175. https://doi.org/10.1021/acs.biomac.0c00583
12. Gerbin E, Rivière GN, Foulon L, et al. (2021) Tuning the functional properties of lignocellulosic films by controlling the molecular and supramolecular structure of lignin. *Int J Biol Macromol* 181: 136–149. https://doi.org/10.1016/j.ijbiomac.2021.03.081
13. Leung C, Kinns H, Hoogenboom BW, et al. (2009) Imaging surface charges of individual biomolecules. *Nano Lett* 9: 2769–2773. https://doi.org/10.1021/nl9012979
14. Seelert H, Poetsch A, Dencher NA, et al. (2000) Structural biology. Proton-powered turbine of a plant motor. *Nature* 405: 418–419. https://doi.org/10.1038/35013148
15. Fotiadis D, Liang Y, Filipek S, et al. (2003) Atomic-force microscopy: Rhodopsin dimers in native disc membranes. *Nature* 421: 127–128. https://doi.org/10.1038/421127a

16. Wong OK, Guthold M, Erie DA, et al. (2008) Interconvertible lac repressor-DNA loops revealed by single-molecule experiments. *PLoS Biol* 6: e232. https://doi.org/10.1371/journal.pbio.0060232
17. Pallarés MC, Marcuello C, Botello-Morte L, et al. (2014) Sequential binding of FurA from Anabaena sp. PCC 7120 to iron boxes: exploring regulation at the nanoscale. *Biochim Biophys Acta* 1844: 623–631. https://doi.org/10.1016/j.bbapap.2014.01.005
18. Nakata E, Dinh H, Nguyen TM, et al. (2019) DNA binding adaptors to assemble proteins of interest on DNA scaffold. *Methods Enzymol* 617: 287–322. https://doi.org/10.1016/bs.mie.2018.12.014
19. Müller DJ and Dufrêne YF (2008) Atomic force microscopy as a multifunctional molecular toolbox in nanobiotechnology. *Nat Nanotechnol* 3: 261–269. https://doi.org/10.1038/nnano.2008.100
20. Allison DP, Hinterdorfer P, Han W (2002) Biomolecular force measurements and the atomic force microscope. *Curr Opin Biotechnol* 13: 47–51. https://doi.org/10.1016/s0958-1669(02)00283-5
21. Müller DJ, Krieg M, Alsteen D, et al. (2009) New frontiers in atomic force microscopy: analyzing interactions from single-molecules to cells. *Curr Opin Biotechnol* 20: 4–13. https://doi.org/10.1016/j.copbio.2009.02.005
22. Rief M, Gautel M, Oesterhelt F, et al. (1997) *Science* 276: 1109–1112. https://doi.org/10.1126/science.273.5315.1109
23. Giganti D, Yan K, Badilla CL, et al. (2018) Disulfide isomerization reactions in titin immunoglobulin domains enable a mode of protein elasticity. *Nat Commun* 9: 185. https://doi.org/10.1038/s41467-017-02528-7
24. Lipiec E, Sofinska K, Seweryn S, et al. (2021) Revealing DNA Structure at Liquid/Solid Interfaces by AFM-Based High-Resolution Imaging and Molecular Spectroscopy. *Molecules* 26: 6476. https://doi.org/10.3390/molecules26216476
25. Liu Y, Tian F, Shi S, et al. (2021) Enzymatic Protein-Protein Conjugation through Internal Site Verified at the Single-Molecule Level. *J Phys Chem Lett* 12: 10914–10919. https://doi.org/10.1021/acs.jpclett.1c02767
26. Lipke PN, Rauceo JM, Viljoen A (2022) Cell-Cell Mating Interactions: Overview and Potential of Single-Cell Force Spectroscopy. *Int J Mol Sci* 23: 1110. https://doi.org/10.3390/ijms23031110
27. Sluysmans D, Lussis P, Fustin C-A, et al. (2021) Real-Time Fluctuations in Single-Molecule Rotaxane Experiments Reveal an Intermediate Weak Binding State during Shuttling. *J Am Chem Soc* 143: 2348–2352. https://doi.org/10.1021/jacs.0c12161
28. Marcuello C, Foulon L, Chabbert B, et al. (2018) Langmuir-Blodgett Procedure to Precisely Control the Coverage of Functionalized AFM Cantilevers for SMFS Measurements: Application with Cellulose Nanocrystals. *Langmuir* 34: 9376–9386. https://doi.org/10.1021/acs.langmuir.8b01892
29. Berzin F, Lemkhanter L, Marcuello C, et al. (2020) Influence of the polarity of the matrix on the breakage mechanisms of lignocellulosic fibers during twin-screw extrusion. *Polym Compos* 41: 1106–11170. https://doi.org/10.1002/pc.25442
30. Dufrêne YF, Ando T, Garcia R, et al. (2017) Imaging modes of atomic force microscopy for application in molecular and cell biology. *Nat Nanotechnol* 12: 295–307. https://doi.org/10.1038/nnano.2017.45

31. Marcuello C, de Miguel R, Gómez-Moreno C, et al. (2012) An efficient method for enzyme immobilization evidenced by atomic force microscopy. *Protein Eng Des Sel* 25: 715–723. https://doi.org/10.1093/protein/gzs086
32. Evans E and Ritchie K (1997) Dynamic strength of molecular adhesion bonds. *Biophys J* 72: 1541–1555. https://doi.org/10.1016/S0006-3495(97)78802-7
33. Marcuello C, de Miguel R, Martínez-Júlvez M, et al. (2015) Mechanostability of the single-electron-transfer complexes of anabaena Ferredoxin-NADP(+) reductase. *Chemphyschem* 16: 3161–3169. https://doi.org/10.1002/cphc.201500534
34. Pérez-Dominguez S, Caballero-Mancebo S, Marcuello C, et al. (2022) Nanomechanical study of enzyme: coenzyme complexes: bipartite sites in plastidic Ferredoxin-NADP$^+$ reductase for the interaction with NADP. *Antioxidants* 11: 537. https://doi.org/10.3390/antiox11030537
35. Fu Y, Wang J, Wang Y, et al. (2022) Investigating the effect of tyrosine kinase inhibitors on the interation between human serum albumin by atomic force microscopy. *Biomolecules* 12: 819. https://doi.org/10.3390/biom12060819
36. Li S, Pang X, Zhao J, et al. (2021) Evaluation the single-molecule interactions between targeted peptides and the receptors on living cell membrane. *Nanoscale* 13: 17318–17324. https://doi.org/10.1039/d1nr05547j
37. Bell GI (1978) Models for the specific adhesion of cells to cells: A theoretical framework for adhesion mediated by reversible bonds between cell surface molecules. *Science* 200: 618–627. https://doi.org/10.1126/science.347575
38. Hänggi P, Talkner P, Borkovec M (1990) Reaction-rate theory: fifty years after Kramers. *Rev Mod Phys* 62: 251–341. https://doi.org/10.1103/RevModPhys.62.251
39. Hummer G and Szabo A (2003) Kinetics from nonequilibrium single-molecule pulling experiments. *Biophys J* 85: 5–15. https://doi.org/10.1016/S0006-3495(03)74449-X
40. Freund LB (2009) Characterizing the resistance generated by a molecular bond as it is forcibly separated. *Proc Natl Acad Sci U S A* 106: 8818–8823. https://doi.org/10.1073/pnas.0903003106
41. Maitra A and Arya G (2010) Model accounting for the effects of pulling-device stiffness in the analyses of single-molecule force measurements. *Phys Rev Lett* 104: 108301. https://doi.org/10.1103/PhysRevLett.104.108301
42. Yoon G, Na S, Eom K (2012) Loading device effect on protein unfolding mechanics. *J Chem Phys* 137: 025102. https://doi.org/10.1063/1.4732798
43. Tapia-Rojo R, Marcuello C, Lostao A, et al. (2017) A physical picture for mechanical dissociation of biological complexes: from forces to free energies. *Phys Chem Chem Phys* 19: 4567–4575. https://doi.org/10.1039/c6cp07508h
44. Priyadharshini RD, Ponkarpagam S, Vennila KN (2022) Multi-spectroscopic and free energy landscape analysis on the binding of antiviral drug remdesivir with calf thymus DNA. *Spectrochim Acta A Mol Biomol Spectrosc* 278: 121363. https://doi.org/10.1016/j.saa.2022.121363
45. Woodside MT and Block SM (2014) Reconstructing folding energy landscapes by single-molecule force spectroscopy. *Annu Rev Biophys* 43: 19–39. https://doi.org/10.1146/annurev-biophys-051013-022754
46. Krieg M, Fläschner G, Alsteens D, et al. (2019) Atomic force microscopy-based mechanobiology. *Nat Rev Phys* 1: 41–57. https://doi.org/10.1038/s42254-018-0001-7

47. Hertz H (1882) Uber die Berührung fester elastischer Körper. *J für die Reine und Angew Math* 92: 156–171. https://doi.org/10.1515/crll.1882.92.156
48. Derjaguin BV, Müller VM, Toporov YP (1975) Effect of contact deformations on the adhesión of particles. *J Colloid Interface Sci* 53: 314–326. https://doi.org/10.1016/0021-9797(75)90018-1
49. Ding Y, Xu G-K, Wang G-F (2017) On the determination of elastic moduli of cells by AFM based indentation. *Sci Rep* 7: 45575. https://doi.org/10.1038/srep45575
50. Freeman KG, Huffman, JB, Homa FL, et al. (2021) UL25 capsid binding facilitates mechanical maturation of the herpesvirus capsid and allows retention of pressurized DNA. *J Virol* 95: e0075521. https://doi.org/10.1128/JVI.00755-21
51. Kwon T, Gunasekaran S, Eom K (2019) Atomic force microscopy-based cancer diagnosis by detecting cancer-specific biomolecules and cells. *Biochim Biophys Acta Rev Cancer* 1871: 367–378. https://doi.org/10.1016/j.bbcan.2019.03.002
52. Marcuello C, Foulon L, Chabbert B, et al. (2020) Atomic force microscopy reveals how relative humidity impacts the Young's modulus of Lignocellulosic polymers at their adhesion with cellulose nanocrystals at the nanoscale. *Int J Biol Macromol* 147: 1064–1075. https://doi.org/10.1016/j.ijbiomac.2019.10.074
53. Joshi J, Homburg SV, Ehrmann A (2022) Atomic Force Microscopy (AFM) on Biopolymers and Hydrogels for Biotechnological Applications-Possibilities and Limits. *Polymers* 14: 1267. https://doi.org/10.3390/polym14061267
54. Naqvi SM and McNamara LM (2020) Stem cell mechanobiology and the role of biomaterials in governing mechanotransduction and matrix production for tissue regeneration. *Front Bioeng Biotechnol* 8: 597661. https://doi.org/10.3389/fbioe.2020.597661
55. Xu H, Guan J, Jin Z, et al. (2022) Mechanical force modulates macrophage proliferation via Piezo1-AKT-Cyclin D1 axis. *FASEB J* 36: 22423. https://doi.org/10.1096/fj.202200314R
56. Li N, Zhang X, Zhou J, et al. (2022) Multiscale biomechanics and mechanotransduction from liver fibrosis to cancer. *Adv Drug Deliv Rev* 188: 114448. https://doi.org/10.1016/j.addr.2022.114448
57. Schot M, Araújo-Gomes N, van Loo B, et al. (2022) Scalable fabrication, compartmentalization and applications of living microtissues. *Bioact Mater* 19: 392–405. https://doi.org/10.1016/j.bioactmat.2022.04.005
58. Dazzi A, Prazares R, Glotin F, et al. (2007) Analysis of nano-chemical mapping performed by an AFM-based ("AFMIR") cousto-optic technique. *Ultramicroscopy* 107: 1194–1200. https://doi.org/10.1016/j.ultramic.2007.01.018
59. Coste R, Soliman M, Bercu NB, et al. (2021) Unveiling the impact of embedding resins on the physicochemical traits of wood cell walls with subcellular functional probing. *Compos Sci Technol* 201: 108485. https://doi.org/10.1016/j.compscitech.2020.108485
60. Nie B, Stutzman J, Xie A (2005) A vibrational spectral marker for probing the hydrogen-bonding status of protonated Asp and Glu residues. *Biophys J* 88: 2833–2847. https://doi.org/10.1529/biophysj.104.047639
61. Giliberti V, Polit R, Ritter E, et al. (2019) Tip-enhanced infrared difference-nanospectroscopy of the proton pump activity of bacteriorhodopsin in single purple membrane patches. *Nano Lett* 19: 3104–3114. https://doi.org/10.1021/acs.nanolett.9b00512

62. Ruggeri FS, Habchi J, Chia S, et al. (2021) Infrared nanospectroscopy reveals the molecular interaction fingerprint of an aggregation inhibitor with single $A\beta_{42}$ oligomers. *Nat Commun* 12: 688. https://doi.org/10.1038/s41467-020-20782-0
63. Dos Santos ACVD, Tranchida D, Lendl B, et al. (2022) Nanoscale chemical characterization of a post-consumer recycled polyolefin blend using tapping mode AFM-IR. *Analyst* 147: 3741–3747. https://doi.org/10.1039/d2an00823h
64. Martin Y and Wickramasinghe K (1987) Magnetic imaging by "force microscopy" with 1000 Å resolution. *Appl Phys Lett* 50: 1455. https://doi.org/10.1063/1.97800
65. Marcuello C, Chambel L, Rodrigues MS, et al. (2018) Magnetotactic Bacteria: Magnetism Beyond Magnetosomes. *IEEE Trans Nanobioscience* 17: 555–559. https://doi.org/10.1109/TNB.2018.2878085
66. Klumpp S, Lefèvre CT, Bennet M, et al. (2019) Swimming with magnets: From biological organisms to synthetic devices. *Phys Rep* 789: 1–54. https://doi.org/10.1016/j.physrep.2018.10.007
67. Moskalenko AV, Yarova PL, Gordeev SN, et al. (2010) Single protein molecule mapping with magnetic atomic force microscopy. *Biophys J* 98: 478–487. https://doi.org/10.1016/j.bpj.2009.10.021
68. Krivcov A, Schneider J, Junkers T, et al. (2019) Magnetic Force Microscopy of in a Polymer Matrix Embedded Single Magnetic Nano Particles. *Phys Status Solidi A* 216: 1800753. https://doi.org/10.1002/pssa.201800753
69. Mantso T, Vasileiadis S, Anestopoulos I, et al. (2018) Hyperthermia induces therapeutic effectiveness and potentiates adjuvant therapy with non-targeted and targeted drugs in an in vitro model of human malignant melanoma. *Sci Rep* 8: 10724. https://doi.org/10.1038/s41598-018-29018-0
70. Mitchell MJ, Billingsley MM, Haley RM, et al. (2021) Engineering precision nanoparticles for drug delivery. *Nat Rev Drug Discov* 20: 101–124. https://doi.org/10.1038/s41573-020-0090-8
71. Pomerantseva E, Bonaccorso F, Feng X, et al. (2019) Energy storage: The future enabled by nanomaterials. *Science* 366: eaan8285. https://doi.org/10.1126/science.aan8285
72. Wang Q, Puerto MC, Warudkar S, et al. (2018) Recyclable amine-functionalized magnetic nanoparticles for efficient demulsification of crude oil-in-water emulsions. *Environ Sci Water Res* 4: 1553–1563. https://doi.org/10.1039/C8EW00188J
73. Marcuello C, Frempong GA, Balsera M, et al. (2021) Atomic force microscopy to elicit conformational transitions of ferredoxin-dependent flavin thioredoxin reductases. *Antioxidants* 10: 1437. https://doi.org/10.3390/antiox10091437
74. Fukuda S and Ando T (2021) Faster high-speed atomic force microscopy for imaging of biomolecular processes. *Rev Sci Instrum* 92: 033705. https://doi.org/10.1063/5.0032948
75. Rico F, Russek A, González L, et al. (2019) Heterogeneous and rate-dependent streptavidin-biotin unbinding revealed by high-speed force spectroscopy and atomistic simulations. *Proc Natl Acad Sci U S A* 14: 6594–6601. https://doi.org/10.1073/pnas.1816909116
76. Marcuello C, de Miguel R, Lostao A (2022) Molecular recognition of proteins through quantitative force maps at single molecule level. *Biomolecules* 12: 594. https://doi.org/10.3390/biom12040594
77. Park J, Yang J, Lee G, et al. (2011) Single-molecule recognition of biomolecular interaction via Kelvin probe force microscopy. *ACS Nano* 5: 6981–6990. https://doi.org/10.1021/nn201540c

78. Chtcheglova LA and Hinterdorfer P (2018) Simultaneous AFM topography and recognition imaging at the plasma membrane of mammalian cells. *Semin Cell Dev Biol* 73: 45–56. https://doi.org/10.1016/j.semcdb.2017.08.025
79. Hwang MT, Heiranian M, Kim Y, et al. (2020) Ultrasensitive detection of nucleic acids using deformed graphene chanel field effect biosensors. *Nat Commun* 11: 1543. https://doi.org/10.1038/s41467-020-15330-9
80. Shim WC, Woo S, Park JW (2022) Nanoscale force-mapping-based quantification of low-abundance methylated DNA. *Nano Lett* 22: 1324–1330. https://doi.org/10.1021/acs.nanolett.1c04637
81. Pascual-Ahuir A, Manzanares-Estreder S, Proft M (2017) Pro-and antioxidant functions of the peroxisome mitochondria connection and its impact on aging and disease. *Oxid Med Cell Longev* 2017: 9860841. https://doi.org/10.1155/2017/9860841
82. Botti V, Marrone S, Cannistraro S, et al. (2022) Interaction between miR4749 and human serum albumin as revealed by fluorescence, FRET, atomic force spectroscopy and computational modeling. *Int J Mol Sci* 23: 1291. https://doi.org/10.3390/ijms23031291
83. Bustamante CJ, Chemla YR, Liu S, et al. (2021) Optical tweezers in single-molecule biophysics. Nat Rev Methods Primers. *Nat Rev Methods Primers* 1: 25. https://doi.org/10.1038/s43586-021-00021-6
84. De Vlaminck I and Dekker C (2012) Recent advances in magnetic tweezers. *Annu Rev Biophys* 41: 453–472. https://doi.org/10.1146/annurev-biophys-122311-100544